Chapter 1
Introduction

In this chapter, we explain what is beamforming, how it works, and introduce beamforming with Kronecker products. Then, we present the organization of this work.

1.1 Beamforming

Beamforming or spatial filtering is an active and central research area of array signal processing [1, 2, 3, 4, 5]. Beamforming algorithms fall into two major categories depending on whether the noise or signal statistics are considered in forming the beamforming filters, i.e., fixed and adaptive beamforming. A fixed beamformer is a spatial filter that has the ability to form a main beam in the direction of the desired signal and, possibly, place nulls in the directions of interferences without the knowledge of the data picked up by the array or the statistics of the desired and noise signals. Accordingly, the coefficients of this filter are fixed and do not depend on the changes of the wave propagation environment in which the array performs. Adaptive beamforming algorithms consider using either the noise statistics or the statistics of the array observation data to optimize the beamforming filters. The performance of adaptive beamforming can be "more" optimal than its fixed counterpart as long as the signal statistics are correctly estimated.

Consider an array of M sensors and assume that a desired signal impinges on this array from the angle θ_{d}, as illustrated in Fig. 1.1. Then, the observation signal vector (of length M) is

$$\begin{aligned}\mathbf{y}(\omega) &= \left[Y_1(\omega) \;\; Y_2(\omega) \;\; \cdots \;\; Y_M(\omega)\right]^T \\ &= \mathbf{d}_{\theta_{\mathrm{d}}}(\omega) X(\omega) + \mathbf{v}(\omega),\end{aligned} \tag{1.1}$$

J. Benesty et al., *Array Processing*, Springer Topics in Signal Processing 18, https://doi.org/10.1007/978-3-030-15600-8_1

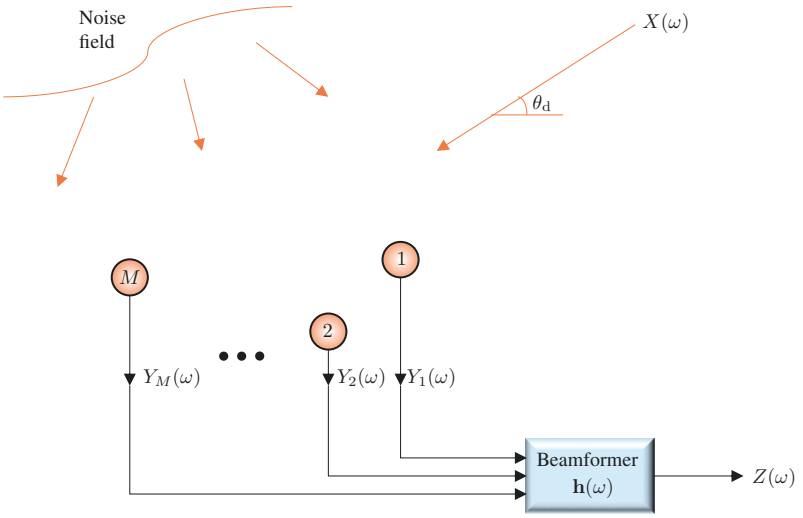

Fig. 1.1 Illustration of an array of M sensors and a beamformer applied to the observation signals.

where ω is the angular frequency, $Y_m(\omega)$ is the mth sensor signal, $X(\omega)$ is the desired source signal, $\mathbf{d}_{\theta_{\mathrm{d}}}(\omega)$ is the steering vector at $\theta = \theta_{\mathrm{d}}$, and $\mathbf{v}(\omega)$ is the additive noise signal vector defined similarly to $\mathbf{y}(\omega)$.

The conventional way of doing beamforming is by applying a complex-valued linear filter, $\mathbf{h}(\omega)$, of length M to the observation signal vector, $\mathbf{y}(\omega)$ [6, 7]. This gives the output:

$$Z(\omega) = \mathbf{h}^H(\omega)\,\mathbf{y}(\omega), \tag{1.2}$$

where $Z(\omega)$ is the estimate of the desired signal, $X(\omega)$. The process of finding the appropriate filter, $\mathbf{h}(\omega)$, based on some given performance criteria is called beamforming.

One of the most useful performance criteria is the beampattern, which describes the sensitivity of the beamformer to a plane wave impinging on the array from the direction θ. Mathematically, it is defined as

$$\mathcal{B}_\theta[\mathbf{h}(\omega)] = \mathbf{d}_\theta^H(\omega)\,\mathbf{h}(\omega). \tag{1.3}$$

A convenient way to evaluate the sensitivity of the array to some of its imperfections, such as sensor noise, is via the so-called white noise gain (WNG), which is given by

$$\mathcal{W}[\mathbf{h}(\omega)] = \frac{\left|\mathbf{h}^H(\omega)\,\mathbf{d}_{\theta_{\mathrm{d}}}(\omega)\right|^2}{\mathbf{h}^H(\omega)\,\mathbf{h}(\omega)}. \tag{1.4}$$

Another important measure, which quantifies how the sensor array performs in the presence of reverberation is the directivity factor (DF), defined as (for linear arrays) [4]

$$\begin{aligned}\mathcal{D}\left[\mathbf{h}\left(\omega\right)\right] &= \frac{\left|\mathcal{B}_{\theta_{\mathrm{d}}}\left[\mathbf{h}\left(\omega\right)\right]\right|^2}{\frac{1}{2}\int_0^{\pi}\left|\mathcal{B}_{\theta}\left[\mathbf{h}\left(\omega\right)\right]\right|^2\sin\theta d\theta} \\ &= \frac{\left|\mathbf{h}^H\left(\omega\right)\mathbf{d}_{\theta_{\mathrm{d}}}\left(\omega\right)\right|^2}{\mathbf{h}^H\left(\omega\right)\mathbf{\Gamma}\left(\omega\right)\mathbf{h}\left(\omega\right)},\end{aligned} \tag{1.5}$$

where

$$\mathbf{\Gamma}\left(\omega\right) = \frac{1}{2}\int_0^{\pi}\mathbf{d}_{\theta}\left(\omega\right)\mathbf{d}_{\theta}^H\left(\omega\right)\sin\theta d\theta. \tag{1.6}$$

With the conventional beamforming approach, M coefficients of $\mathbf{h}\left(\omega\right)$ need to be estimated. Here, we are interested in arrays of $M = M_1M_2$ sensors that enable to decompose the steering vector as a Kronecker product of two steering vectors of smaller virtual arrays [8, 9, 10]. That is, the steering vector (of length M) is decomposed as

$$\mathbf{d}_{\theta}\left(\omega\right) = \mathbf{d}_{1,\theta}\left(\omega\right)\otimes\mathbf{d}_{2,\theta}\left(\omega\right), \tag{1.7}$$

where $\otimes$ is the Kronecker product, $\mathbf{d}_{1,\theta}\left(\omega\right)$ is the steering vector (of length M_1) corresponding to a virtual array of M_1 sensors, and $\mathbf{d}_{2,\theta}\left(\omega\right)$ is the steering vector (of length M_2) corresponding to another virtual array of M_2 sensors.

Figure 1.2 shows examples of Kronecker product decompositions of a uniform linear array (ULA) of 12 sensors with an interelement spacing equal to δ into two smaller virtual ULAs with different numbers of sensors and different interelement spacings. Note that (1.7) is satisfied whenever the global array can be obtained from replications of one virtual array to the sensor positions of the other virtual array. Figure 1.3 shows examples of Kronecker product decompositions of a nonuniform linear array (NULA) of 12 sensors into two smaller virtual ULAs. Figure 1.4 shows examples of Kronecker product decompositions of a two-dimensional rectangular array (RA) of 24 sensors into ULAs and RAs with different numbers of sensors and different interelement spacings.

In the proposed approach, instead of directly designing the filter $\mathbf{h}\left(\omega\right)$ of length M, we break it down following the decomposition of the global steering vector as

$$\mathbf{h}\left(\omega\right) = \mathbf{h}_1\left(\omega\right)\otimes\mathbf{h}_2\left(\omega\right), \tag{1.8}$$

where $\mathbf{h}_1\left(\omega\right)$ and $\mathbf{h}_2\left(\omega\right)$ are two complex-valued linear filters of length M_1 and M_2, respectively. With this method, we only need to estimate $M_1 + M_2$

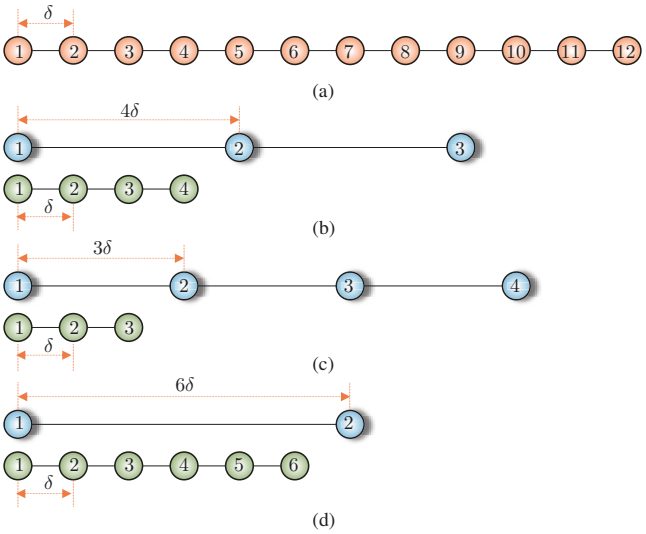

Fig. 1.2 Examples of Kronecker product decompositions of a ULA into two smaller virtual ULAs: (a) a ULA of 12 sensors with an interelement spacing equal to δ; (b) one virtual ULA of 3 sensors with an interelement spacing equal to 4δ, and another virtual ULA of 4 sensors with an interelement spacing equal to δ; (c) one virtual ULA of 4 sensors with an interelement spacing equal to 3δ, and another virtual ULA of 3 sensors with an interelement spacing equal to δ; and (d) one virtual ULA of 2 sensors with an interelement spacing equal to 6δ, and another virtual ULA of 6 sensors with an interelement spacing equal to δ.

coefficients [M_1 for $\mathbf{h}_1(\omega)$ and M_2 for $\mathbf{h}_2(\omega)$] instead of $M = M_1 M_2$ for the conventional technique. This implies smaller matrices to invert (increasing robustness) and less observations to estimate the statistics when necessary.

There are many ways to optimize the coefficients of $\mathbf{h}_1(\omega)$ and $\mathbf{h}_2(\omega)$ depending on what we want and the application at hand. We introduce fixed and adaptive Kronecker product beamformers, and show how to derive such beamformers, as well as new approaches through the design of $\mathbf{h}_1(\omega)$ and $\mathbf{h}_2(\omega)$. We also show how to combine very intelligently fixed and adaptive beamformers, so that the best of each one of these two approaches is emphasized for performance enhancement.

The decomposition (1.8) enables to perform beamforming differently from the well-known and studied conventional approach. In our context, the global beampattern can be expressed as the product of two beamformer beampatterns:

$$\mathcal{B}_\theta\left[\mathbf{h}(\omega)\right] = \mathcal{B}_{1,\theta}\left[\mathbf{h}_1(\omega)\right] \times \mathcal{B}_{2,\theta}\left[\mathbf{h}_2(\omega)\right], \tag{1.9}$$

where

$$\mathcal{B}_{1,\theta}\left[\mathbf{h}_1(\omega)\right] = \mathbf{d}_{1,\theta}^H(\omega)\,\mathbf{h}_1(\omega) \tag{1.10}$$

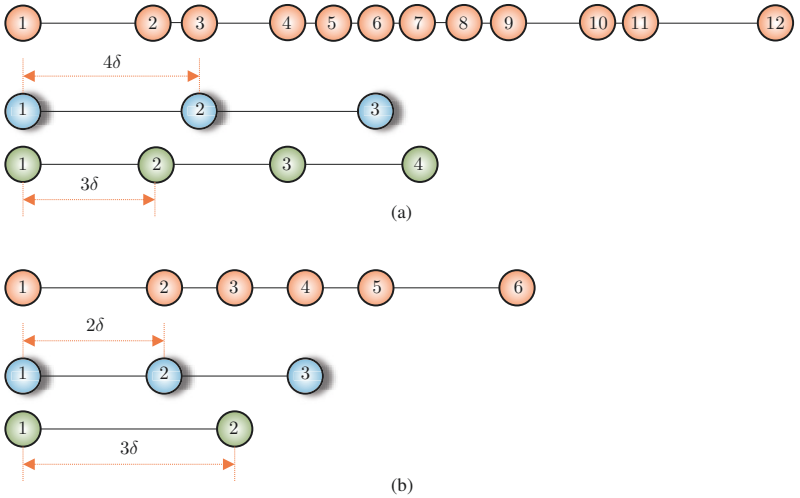

Fig. 1.3 Examples of Kronecker product decompositions of a NULA into two smaller virtual ULAs: (a) a nonuniform linear array of 12 sensors, one virtual ULA of 3 sensors with an interelement spacing equal to 4δ, and another virtual ULA of 4 sensors with an interelement spacing equal to 3δ; and (b) a nonuniform linear array of 6 sensors, one virtual ULA of 3 sensors with an interelement spacing equal to 2δ, and another virtual ULA of 2 sensors with an interelement spacing equal to 3δ.

is the beampattern of the first virtual array, and

$$\mathcal{B}_{2,\theta}\left[\mathbf{h}_2\left(\omega\right)\right] = \mathbf{d}_{2,\theta}^H\left(\omega\right)\mathbf{h}_2\left(\omega\right) \tag{1.11}$$

is the beampattern of the second virtual array. Also, the WNG of the global array can be expressed as the product of the WNGs of the first and second virtual arrays, while the DF of the global array cannot be factorized as the product of the DFs of the two virtual ULAs, i.e.,

$$\mathcal{W}\left[\mathbf{h}\left(\omega\right)\right] = \mathcal{W}_1\left[\mathbf{h}_1\left(\omega\right)\right] \times \mathcal{W}_2\left[\mathbf{h}_2\left(\omega\right)\right], \tag{1.12}$$

$$\mathcal{D}\left[\mathbf{h}\left(\omega\right)\right] \neq \mathcal{D}_1\left[\mathbf{h}_1\left(\omega\right)\right] \times \mathcal{D}_2\left[\mathbf{h}_2\left(\omega\right)\right]. \tag{1.13}$$

These interesting properties can be exploited in the design of very flexible global beamformers.

1.2 Organization of the Work

The material in this book is organized into seven chapters, including this one.

In Chapter 2, we formulate the problem of Kronecker product beamforming with ULAs. We define some important performance measures in this

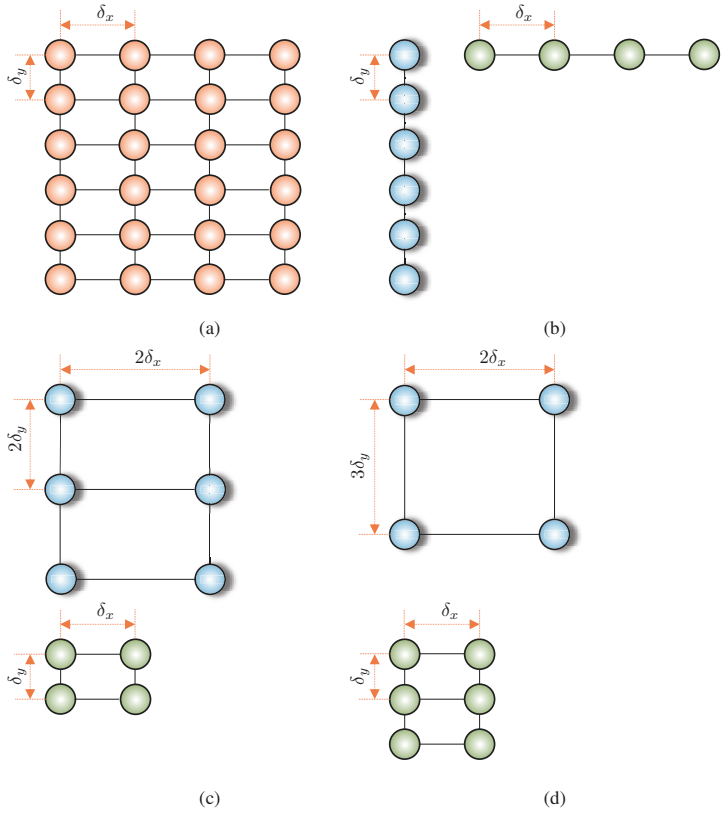

Fig. 1.4 Examples of Kronecker product decompositions of an RA into two smaller virtual arrays: (a) an RA of 24 sensors with an interelement spacing equal to δ_x along the x axis and an interelement spacing equal to δ_y along the y axis; (b) one virtual ULA of 6 sensors with an interelement spacing equal to δ_y and another virtual ULA of 4 sensors with an interelement spacing equal to δ_x; (c) one virtual RA of 2×3 sensors with an interelement spacing equal to $2\delta_x$ along the x axis and an interelement spacing equal to $2\delta_y$ along the y axis, and another virtual RA of 2×2 sensors with an interelement spacing equal to δ_x along the x axis and an interelement spacing equal to δ_y along the y axis; and (d) one virtual RA of 2×2 sensors with an interelement spacing equal to $2\delta_x$ along the x axis and an interelement spacing equal to $3\delta_y$ along the y axis, and another virtual RA of 2×3 sensors with an interelement spacing equal to δ_x along the x axis and an interelement spacing equal to δ_y along the y axis.

context, and explain how to perform beamforming with Kronecker product filters differently from the well-known and studied conventional approach.

In Chapter 3, we show how to derive fixed, adaptive, and differential beamformers with remarkable flexibility thanks to the Kronecker product formulation. We also introduce new beamforming approaches that combine fixed and adaptive beamformers, so that the best of each one of these two approaches is emphasized for performance enhancement.

In Chapter 4, we generalize the Kronecker product beamforming with other decompositions of the steering vector associated with ULAs. We show how to design important differential beamformers, in a very elegant way, thanks to the Kronecker product decompositions of the steering vector and the proposed filtering approach.

The focus of Chapter 5 is on NULAs. We show how from two virtual ULAs we can construct a physical NULA whose associated steering vector is the Kronecker product of the steering vectors associated with the virtual arrays. Then, we explain how Kronecker product beamforming is performed and derive some interesting optimal beamformers.

Chapter 6 continues the investigation of Kronecker product beamforming, but with two-dimensional arrays. Conventional two-dimensional beamforming methods suffer from the need to invert very ill-conditioned large matrices, which necessarily lead to serious estimation problems in the presence of uncertainties. We show how to avoid this problem with Kronecker product beamforming, and how to extend some of the results obtained in previous chapters to two-dimensional arrays such as the rectangular ones.

Finally, in Chapter 7, we address the problem of spatiotemporal signal enhancement with any array geometry. We show how the Kronecker product appears naturally in the definition of the signal vector by taking into account the interframe correlation. We derive spatiotemporal Kronecker product filters, and explain how to perform noise reduction with the most well-known performance measures.

References

1. J. Benesty, J. Chen, and Y. Huang, *Microphone Array Signal Processing*. Berlin, Germany: Springer-Verlag, 2008.
2. J. Benesty, I. Cohen, and J. Chen, *Fundamentals of Signal Enhancement and Array Signal Processing*. Singapore: Wiley–IEEE Press, 2018.
3. S. Haykin and K. J. R. Liu, *Handbook on Array Processing and Sensor Networks*. Hoboken, NJ: Wiley & Sons, 2010.
4. H. L. Van Trees, *Detection, Estimation, and Modulation Theory, Optimum Array Processing* (Part IV). Hoboken, NJ: Wiley-Interscience, 2002.
5. D. H. Johnson and D. E. Dudgeon, *Array Signal Processing: Concepts and Techniques*. Upper Saddle River, NJ: Prentice Hall, 1993.
6. S. Haykin, *Array Signal Processing*. Upper Saddle River, NJ: Prentice-Hall, 1984.
7. H. Krim and M. Viberg, "Two decades of array signal processing research: the parametric approach," *IEEE Signal Process. Mag.*, vol. 13, pp.67–94, Jul. 1996.
8. Y. I. Abramovich, G. J. Frazer, and B. A. Johnson, "Iterative adaptive Kronecker MIMO radar beamformer: description and convergence analysis," *IEEE Trans. Signal Process.*, vol. 58, pp. 3681–3691, Jul. 2010.
9. F. P. Ribeiro and V. H. Nascimento, "Fast transforms for acoustic imaging–Part I: Theory," *IEEE Trans. Image Process.*, vol. 20, pp. 2229–2240, Aug. 2011.
10. B. Masiero and V. H. Nascimento, "Revisiting the Kronecker array transform," *IEEE Signal Process. Lett.*, vol. 24, pp. 525–529, May 2017.

Chapter 2
Problem Formulation with Uniform Linear Arrays

In this chapter, we describe ULAs and define the associated steering vector. In one very particular case, we explain how this vector can be decomposed as a Kronecker product of two steering vectors of smaller ULAs with the same number of elements. Thanks to this decomposition, we explain how to perform beamforming with Kronecker product filters. Then, we derive some very important and useful performance measures in this context that will be of great help to design and evaluate all kind of beamformers.

2.1 Signal Model

We consider a ULA consisting of $M = M_0^2$ omnidirectional microphones, where $M_0 \geq 2$, with an interelement spacing equal to δ. Typical and practical values of M are 4, 9, 16, and even 25. We will refer to this array as the global or whole ULA. Now, assume that a farfield desired source signal (plane wave) propagates from the azimuth angle, θ, in an anechoic acoustic environment at the speed of sound, i.e., $c = 340$ m/s, and impinges on the above described microphone array (see Fig. 2.1). Then, the corresponding steering vector (of length M) is [1], [2]

$$\mathbf{d}_\theta(\omega) = \left[1 \;\; e^{-\jmath\varpi(\theta)} \;\; e^{-\jmath 2\varpi(\theta)} \;\; \cdots \;\; e^{-\jmath(M-1)\varpi(\theta)}\right]^T, \tag{2.1}$$

where the superscript ^{T} is the transpose operator, $\jmath$ is the imaginary unit,

$$\varpi(\theta) = \frac{\omega\delta\cos\theta}{c}, \tag{2.2}$$

$\omega = 2\pi f$ is the angular frequency, and $f > 0$ is the temporal frequency. Since $\cos\theta$ is an even function so is $\mathbf{d}_\theta(\omega)$. Therefore, the study with linear arrays is limited to angles $\theta \in [0, \pi]$.

J. Benesty et al., *Array Processing*, Springer Topics in Signal Processing 18, https://doi.org/10.1007/978-3-030-15600-8_2

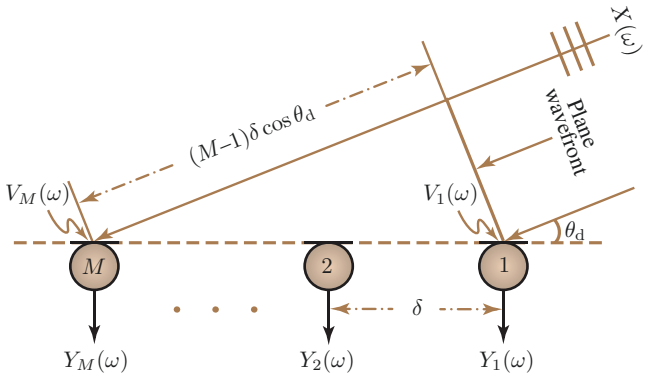

Fig. 2.1 A uniform linear array with M sensors.

The very interesting Vandermonde structure of the vector $\mathbf{d}_\theta(\omega)$ can be exploited. Indeed, it is easy to see that this steering vector can be decomposed as

$$\mathbf{d}_\theta(\omega) = \mathbf{d}_{1,\theta}(\omega) \otimes \mathbf{d}_{2,\theta}(\omega), \tag{2.3}$$

where $\otimes$ is the Kronecker product,

$$\mathbf{d}_{1,\theta}(\omega) = \left[1 \;\; e^{-\jmath M_0 \varpi(\theta)} \;\; e^{-\jmath 2 M_0 \varpi(\theta)} \;\; \cdots \;\; e^{-\jmath M_0 (M_0-1)\varpi(\theta)}\right]^T \tag{2.4}$$

is the steering vector (of length M_0) corresponding to a ULA of M_0 sensors with an interelement spacing equal to $M_0\delta$, and

$$\mathbf{d}_{2,\theta}(\omega) = \left[1 \;\; e^{-\jmath \varpi(\theta)} \;\; e^{-\jmath 2 \varpi(\theta)} \;\; \cdots \;\; e^{-\jmath (M_0-1)\varpi(\theta)}\right]^T \tag{2.5}$$

is the steering vector (of length M_0) corresponding also to a ULA of M_0 sensors but with an interelement spacing equal to δ. In fact, the components of $\mathbf{d}_{2,\theta}(\omega)$ are identical to the first M_0 elements of $\mathbf{d}_\theta(\omega)$. We will refer to these two arrays as the first and second ULAs or the subarrays. In the design of beamformers or beampatterns, it is important to keep in mind that the second ULA is much less sensitive to spatial aliasing than the first one since $\delta \ll M_0\delta$. To summarize, we can state that, when $M = M_0^2$, the steering vector (of length M_0^2) associated with the global ULA is simply the Kronecker product of the steering vectors (of length M_0) associated with the first and second ULAs.

Assume that the desired signal propagates from the angle $\theta_{\rm d}$. Then, the observation signal vector (of length M) is [3], [4]

$$\begin{aligned}\mathbf{y}(\omega) &= \left[Y_1(\omega) \;\; Y_2(\omega) \;\; \cdots \;\; Y_M(\omega) \right]^T \\ &= \mathbf{x}(\omega) + \mathbf{v}(\omega) \\ &= \mathbf{d}_{\theta_\mathrm{d}}(\omega) X(\omega) + \mathbf{v}(\omega), \end{aligned} \tag{2.6}$$

where $Y_m(\omega)$ is the mth microphone signal, $\mathbf{x}(\omega) = \mathbf{d}_{\theta_\mathrm{d}}(\omega) X(\omega)$, $X(\omega)$ is the zero-mean desired source signal, $\mathbf{d}_{\theta_\mathrm{d}}(\omega) = \mathbf{d}_{1,\theta_\mathrm{d}}(\omega) \otimes \mathbf{d}_{2,\theta_\mathrm{d}}(\omega)$ is the steering vector at $\theta = \theta_\mathrm{d}$ (direction of the desired source), $\mathbf{v}(\omega)$ is the zero-mean additive noise signal vector defined similarly to $\mathbf{y}(\omega)$, and $X(\omega)$ and $\mathbf{v}(\omega)$ are uncorrelated. In the rest, in order to simplify the notation, we drop the dependence on the angular frequency, ω. So, for example, (2.6) is written as $\mathbf{y} = \mathbf{d}_{\theta_\mathrm{d}} X + \mathbf{v}$. We deduce that the covariance matrix of $\mathbf{y}$ is

$$\begin{aligned}\mathbf{\Phi}_\mathbf{y} &= E\left(\mathbf{y}\mathbf{y}^H\right) \\ &= \mathbf{\Phi}_\mathbf{x} + \mathbf{\Phi}_\mathbf{v}, \end{aligned} \tag{2.7}$$

where $E(\cdot)$ denotes mathematical expectation, the superscript ^{H} is the conjugate-transpose operator,

$$\begin{aligned}\mathbf{\Phi}_\mathbf{x} &= \phi_X \mathbf{d}_{\theta_\mathrm{d}} \mathbf{d}_{\theta_\mathrm{d}}^H \\ &= \phi_X \left(\mathbf{d}_{1,\theta_\mathrm{d}} \otimes \mathbf{d}_{2,\theta_\mathrm{d}}\right) \left(\mathbf{d}_{1,\theta_\mathrm{d}} \otimes \mathbf{d}_{2,\theta_\mathrm{d}}\right)^H \\ &= \phi_X \left(\mathbf{d}_{1,\theta_\mathrm{d}} \mathbf{d}_{1,\theta_\mathrm{d}}^H\right) \otimes \left(\mathbf{d}_{2,\theta_\mathrm{d}} \mathbf{d}_{2,\theta_\mathrm{d}}^H\right) \end{aligned} \tag{2.8}$$

is the covariance matrix of $\mathbf{x}$, with $\phi_X = E\left(|X|^2\right)$ being the variance of X, and $\mathbf{\Phi}_\mathbf{v} = E\left(\mathbf{v}\mathbf{v}^H\right)$ is the covariance matrix of $\mathbf{v}$. Assuming that the first sensor is the reference, we can express (2.7) as

$$\mathbf{\Phi}_\mathbf{y} = \phi_X \mathbf{d}_{\theta_\mathrm{d}} \mathbf{d}_{\theta_\mathrm{d}}^H + \phi_{V_1} \mathbf{\Gamma}_\mathbf{v}, \tag{2.9}$$

where $\phi_{V_1} = E\left(|V_1|^2\right)$ is the variance of the noise at the reference sensor and $\mathbf{\Gamma}_\mathbf{v} = \mathbf{\Phi}_\mathbf{v}/\phi_{V_1}$ is the pseudo-coherence matrix of the noise. In the case of the spherically isotropic (diffuse) noise field, which will be assumed in fixed beamforming, (2.9) becomes

$$\mathbf{\Phi}_\mathbf{y} = \phi_X \mathbf{d}_{\theta_\mathrm{d}} \mathbf{d}_{\theta_\mathrm{d}}^H + \phi \mathbf{\Gamma}, \tag{2.10}$$

where ϕ is the variance of the diffuse noise and

$$\mathbf{\Gamma} = \frac{1}{2} \int_0^\pi \mathbf{d}_\theta \mathbf{d}_\theta^H \sin\theta d\theta. \tag{2.11}$$

It can be verified that the elements of the $M \times M$ matrix $\mathbf{\Gamma}(\omega)$ are

$$[\mathbf{\Gamma}(\omega)]_{ij} = \frac{\sin[\omega(j-i)\delta/c]}{\omega(j-i)\delta/c} = \operatorname{sinc}[\omega(j-i)\delta/c], \tag{2.12}$$

with $[\mathbf{\Gamma}(\omega)]_{mm} = 1,\ m = 1, 2, \ldots, M$.

One of our main objectives in this study is to take advantage of the global ULA steering vector structure in the particular case of $M = M_0^2$ to perform beamforming differently from the well-known and studied conventional approach. It will be demonstrated that the new technique is extremely flexible.

2.2 Beamforming with Kronecker Product Filters

The conventional way of doing beamforming is by applying a complex-valued linear filter, $\mathbf{h}_{\mathrm{C}}$, of length M to the observation signal vector, $\mathbf{y}$. This processing is [4]

$$Z_{\mathrm{C}} = \mathbf{h}_{\mathrm{C}}^H \mathbf{y}, \tag{2.13}$$

where Z_{C} is the estimate of the desired signal, X. While this approach is optimal as far as linear filtering is concerned, it lacks flexibility and M_0^2 coefficients of $\mathbf{h}_{\mathrm{C}}$ need to be estimated.

In order to fully exploit the structure of the global steering vector, let us consider the $M \times 1$ complex-valued filters having the form:

$$\mathbf{h} = \mathbf{h}_1 \otimes \mathbf{h}_2, \tag{2.14}$$

where $\mathbf{h}_1$ and $\mathbf{h}_2$ are two complex-valued linear filters of length M_0. In other words, the global beamformer, $\mathbf{h}$, follows the decomposition of the global steering vector, $\mathbf{d}_\theta$. In the proposed approach, beamforming is performed by applying $\mathbf{h}$ [as defined in (2.14)] to $\mathbf{y}$ [from (2.6)]. We get

$$\begin{aligned} Z &= \mathbf{h}^H \mathbf{y} \\ &= \mathbf{h}^H \mathbf{d}_{\theta_{\mathrm{d}}} X + \mathbf{h}^H \mathbf{v} \\ &= X_{\mathrm{fd}} + V_{\mathrm{rn}}, \end{aligned} \tag{2.15}$$

where Z is the estimate of the desired signal, X,

$$\begin{aligned} X_{\mathrm{fd}} &= (\mathbf{h}_1 \otimes \mathbf{h}_2)^H (\mathbf{d}_{1,\theta_{\mathrm{d}}} \otimes \mathbf{d}_{2,\theta_{\mathrm{d}}}) X \\ &= \left(\mathbf{h}_1^H \mathbf{d}_{1,\theta_{\mathrm{d}}}\right)\left(\mathbf{h}_2^H \mathbf{d}_{2,\theta_{\mathrm{d}}}\right) X \end{aligned} \tag{2.16}$$

is the filtered desired signal, and

$$V_{\mathrm{rn}} = (\mathbf{h}_1 \otimes \mathbf{h}_2)^H \mathbf{v} \tag{2.17}$$

is the residual noise. We deduce that the variance of Z is

$$\phi_Z = \phi_X \left|\mathbf{h}_1^H \mathbf{d}_{1,\theta_\mathrm{d}}\right|^2 \left|\mathbf{h}_2^H \mathbf{d}_{2,\theta_\mathrm{d}}\right|^2 + \phi_{V_1} \left(\mathbf{h}_1 \otimes \mathbf{h}_2\right)^H \mathbf{\Gamma}_\mathbf{v} \left(\mathbf{h}_1 \otimes \mathbf{h}_2\right). \tag{2.18}$$

We see that with this method, we only need to estimate $2M_0$ coefficients (M_0 for $\mathbf{h}_1$ and M_0 for $\mathbf{h}_2$) instead of M_0^2 for the conventional technique. This implies smaller matrices to invert (increasing robustness) and less observations to estimate the statistics when necessary. Notice that this way of doing beamforming may not be completely new. A similar approach was proposed in [5] but in the context of MIMO radar applications and in a rather very limited way.

In our context, the distortionless constraint in the direction of the desired source, i.e., $\theta = \theta_\mathrm{d}$, is often required, i.e.,

$$\mathbf{h}^H \mathbf{d}_{\theta_\mathrm{d}} = \left(\mathbf{h}_1^H \mathbf{d}_{1,\theta_\mathrm{d}}\right) \left(\mathbf{h}_2^H \mathbf{d}_{2,\theta_\mathrm{d}}\right) = 1. \tag{2.19}$$

Therefore, we will often (if not always) choose $\mathbf{h}_1^H \mathbf{d}_{1,\theta_\mathrm{d}} = \mathbf{h}_2^H \mathbf{d}_{2,\theta_\mathrm{d}} = 1$, so that (2.19) is satisfied.

2.3 Performance Measures

We are going to define some important performance measures by using Kronecker product filters. It will be shown how flexibility appears thanks to this decomposition.

The first useful measure discussed in this section is the beampattern or directivity pattern, which describes the sensitivity of the beamformer to a plane wave (source signal) impinging on the global ULA from the direction θ. Mathematically, it is defined as

$$\begin{aligned} \mathcal{B}_\theta\left(\mathbf{h}\right) &= \mathbf{d}_\theta^H \mathbf{h} \\ &= \left(\mathbf{d}_{1,\theta}^H \mathbf{h}_1\right) \left(\mathbf{d}_{2,\theta}^H \mathbf{h}_2\right) \\ &= \mathcal{B}_{1,\theta}\left(\mathbf{h}_1\right) \times \mathcal{B}_{2,\theta}\left(\mathbf{h}_2\right), \end{aligned} \tag{2.20}$$

where

$$\begin{aligned} \mathcal{B}_{1,\theta}\left(\mathbf{h}_1\right) &= \mathbf{d}_{1,\theta}^H \mathbf{h}_1 \\ &= \sum_{m=1}^{M_0} H_{1,m} e^{\jmath(m-1)M_0 \varpi(\theta)} \end{aligned} \tag{2.21}$$

is the beampattern of the first ULA, with $H_{1,m},\ m = 1, 2, \ldots, M_0$ being the coefficients of $\mathbf{h}_1$, and

$$\begin{aligned}\mathcal{B}_{2,\theta}(\mathbf{h}_2) &= \mathbf{d}_{2,\theta}^H \mathbf{h}_2 \\ &= \sum_{m=1}^{M_0} H_{2,m} e^{\jmath(m-1)\varpi(\theta)}\end{aligned} \tag{2.22}$$

is the beampattern of the second ULA, with $H_{2,m},\ m = 1, 2, \ldots, M_0$ being the coefficients of $\mathbf{h}_2$. Let $\mathcal{Z}_1 = e^{\jmath M_0 \varpi(\theta)}$ and $\mathcal{Z}_2 = e^{\jmath\varpi(\theta)}$, we can express the global beampattern as a polynomial in two variables, which is the product of two polynomials (of degree $M_0 - 1$) in one variable each, i.e.,

$$\begin{aligned}\mathcal{B}(\mathcal{Z}_1, \mathcal{Z}_2) &= \mathcal{B}_1(\mathcal{Z}_1) \times \mathcal{B}_2(\mathcal{Z}_2) \\ &= \left(\sum_{m_1=1}^{M_0} H_{1,m_1} \mathcal{Z}_1^{m_1-1}\right)\left(\sum_{m_2=1}^{M_0} H_{2,m_2} \mathcal{Z}_2^{m_2-1}\right).\end{aligned} \tag{2.23}$$

From this perspective, we can see that this beampattern has at most $2(M_0-1)$ distinct nulls (between 0 and π), while the beampattern with the conventional approach has at most $M_0^2 - 1$ distinct nulls (between 0 and π). The fact that the global beampattern, $\mathcal{B}_\theta(\mathbf{h})$, can be expressed as the product of two beamformer beampatterns is an interesting property that can be exploited in the design of very flexible global beamformers.

Given that the first sensor is the reference, we can define the input signal-to-noise ratio (SNR) with respect to this reference as

$$\text{iSNR} = \frac{\phi_X}{\phi_{V_1}}. \tag{2.24}$$

The output SNR is defined [from the variance of Z, see (2.18)] as

$$\begin{aligned}\text{oSNR}(\mathbf{h}) &= \phi_X \frac{\left|\mathbf{h}^H \mathbf{d}_{\theta_\text{d}}\right|^2}{\mathbf{h}^H \mathbf{\Phi}_\mathbf{v} \mathbf{h}} \\ &= \frac{\phi_X}{\phi_{V_1}} \times \frac{\left|\mathbf{h}^H \mathbf{d}_{\theta_\text{d}}\right|^2}{\mathbf{h}^H \mathbf{\Gamma}_\mathbf{v} \mathbf{h}}.\end{aligned} \tag{2.25}$$

The definition of the gain in SNR is obtained from the previous definitions, i.e.,

$$\begin{aligned}\mathcal{G}(\mathbf{h}) &= \frac{\text{oSNR}(\mathbf{h})}{\text{iSNR}} \\ &= \frac{\left|\mathbf{h}^H \mathbf{d}_{\theta_\text{d}}\right|^2}{\mathbf{h}^H \mathbf{\Gamma}_\mathbf{v} \mathbf{h}}.\end{aligned} \tag{2.26}$$

One convenient way to evaluate the sensitivity of the global ULA to some of its imperfections is via the so-called white noise gain (WNG), which is defined by taking $\mathbf{\Gamma}_\mathbf{v} = \mathbf{I}_M$ in (2.26), where $\mathbf{I}_M$ is the $M \times M$ identity matrix, i.e.,

$$\begin{aligned}\mathcal{W}(\mathbf{h}) &= \frac{\left|\mathbf{h}^H \mathbf{d}_{\theta_\mathrm{d}}\right|^2}{\mathbf{h}^H \mathbf{h}} \\ &= \frac{\left|\mathbf{h}_1^H \mathbf{d}_{1,\theta_\mathrm{d}}\right|^2}{\mathbf{h}_1^H \mathbf{h}_1} \times \frac{\left|\mathbf{h}_2^H \mathbf{d}_{2,\theta_\mathrm{d}}\right|^2}{\mathbf{h}_2^H \mathbf{h}_2} \\ &= \mathcal{W}_1(\mathbf{h}_1) \times \mathcal{W}_2(\mathbf{h}_2),\end{aligned} \tag{2.27}$$

where

$$\mathcal{W}_1(\mathbf{h}_1) = \frac{\left|\mathbf{h}_1^H \mathbf{d}_{1,\theta_\mathrm{d}}\right|^2}{\mathbf{h}_1^H \mathbf{h}_1} \tag{2.28}$$

and

$$\mathcal{W}_2(\mathbf{h}_2) = \frac{\left|\mathbf{h}_2^H \mathbf{d}_{2,\theta_\mathrm{d}}\right|^2}{\mathbf{h}_2^H \mathbf{h}_2}. \tag{2.29}$$

Obviously, the WNG of the global ULA is simply the product of the WNGs of the first and second ULAs described in Section 2.1. It is easy to check that

$$\mathcal{W}(\mathbf{h}) \leq M, \ \forall \mathbf{h}. \tag{2.30}$$

Another important measure, which quantifies how the microphone array performs in the presence of spatial acoustic noise and reverberation is the directivity factor (DF). Considering the spherically isotropic (diffuse) noise field, the DF is defined as [6]

$$\begin{aligned}\mathcal{D}(\mathbf{h}) &= \frac{\left|\mathcal{B}_{\theta_\mathrm{d}}(\mathbf{h})\right|^2}{\frac{1}{2}\int_0^\pi \left|\mathcal{B}_\theta(\mathbf{h})\right|^2 \sin\theta d\theta} \\ &= \frac{\left|\mathcal{B}_{1,\theta_\mathrm{d}}(\mathbf{h}_1)\right|^2 \left|\mathcal{B}_{2,\theta_\mathrm{d}}(\mathbf{h}_2)\right|^2}{\frac{1}{2}\int_0^\pi \left|\mathcal{B}_{1,\theta}(\mathbf{h}_1)\right|^2 \left|\mathcal{B}_{2,\theta}(\mathbf{h}_2)\right|^2 \sin\theta d\theta} \\ &= \frac{\left|\mathbf{h}^H \mathbf{d}_{\theta_\mathrm{d}}\right|^2}{\mathbf{h}^H \mathbf{\Gamma} \mathbf{h}},\end{aligned} \tag{2.31}$$

where $\mathbf{\Gamma}$ is defined in (2.11). It is clear that

$$\mathcal{D}(\mathbf{h}) \leq \mathbf{d}_{\theta_\mathrm{d}}^H \mathbf{\Gamma}^{-1} \mathbf{d}_{\theta_\mathrm{d}}, \ \forall \mathbf{h}. \tag{2.32}$$

We observe that contrary to the beampattern and the WNG, the DF of the global ULA cannot be factorized, i.e.,

$$\mathcal{D}(\mathbf{h}) \neq \mathcal{D}_1(\mathbf{h}_1) \times \mathcal{D}_2(\mathbf{h}_2), \tag{2.33}$$

where

$$\mathcal{D}_1(\mathbf{h}_1) = \frac{|\mathcal{B}_{1,\theta_\mathrm{d}}(\mathbf{h}_1)|^2}{\frac{1}{2}\int_0^\pi |\mathcal{B}_{1,\theta}(\mathbf{h}_1)|^2 \sin\theta d\theta} \tag{2.34}$$

$$= \frac{\left|\mathbf{h}_1^H \mathbf{d}_{1,\theta_\mathrm{d}}\right|^2}{\mathbf{h}_1^H \mathbf{\Gamma}_1 \mathbf{h}_1},$$

$$\mathcal{D}_2(\mathbf{h}_2) = \frac{|\mathcal{B}_{2,\theta_\mathrm{d}}(\mathbf{h}_2)|^2}{\frac{1}{2}\int_0^\pi |\mathcal{B}_{2,\theta}(\mathbf{h}_2)|^2 \sin\theta d\theta} \tag{2.35}$$

$$= \frac{\left|\mathbf{h}_2^H \mathbf{d}_{2,\theta_\mathrm{d}}\right|^2}{\mathbf{h}_2^H \mathbf{\Gamma}_2 \mathbf{h}_2},$$

with

$$\mathbf{\Gamma}_1 = \frac{1}{2}\int_0^\pi \mathbf{d}_{1,\theta}\mathbf{d}_{1,\theta}^H \sin\theta d\theta, \tag{2.36}$$

$$\mathbf{\Gamma}_2 = \frac{1}{2}\int_0^\pi \mathbf{d}_{2,\theta}\mathbf{d}_{2,\theta}^H \sin\theta d\theta. \tag{2.37}$$

The elements of the $M_0 \times M_0$ matrices $\mathbf{\Gamma}_1(\omega)$ and $\mathbf{\Gamma}_2(\omega)$ are given, respectively, by

$$[\mathbf{\Gamma}_1(\omega)]_{ij} = \mathrm{sinc}\left[\omega(j-i)M_0\delta/c\right] \tag{2.38}$$

and

$$[\mathbf{\Gamma}_2(\omega)]_{ij} = \mathrm{sinc}\left[\omega(j-i)\delta/c\right], \tag{2.39}$$

with $[\mathbf{\Gamma}_1(\omega)]_{mm} = [\mathbf{\Gamma}_2(\omega)]_{mm} = 1,\ m = 1, 2, \ldots, M_0$. In fact, one can verify that $\mathbf{\Gamma} \neq \mathbf{\Gamma}_1 \otimes \mathbf{\Gamma}_2$, that is why (2.33) is true in general.

One can check that

$$\mathbf{h}_1 \otimes \mathbf{h}_2 = (\mathbf{h}_1 \otimes \mathbf{I}_{M_0})\,\mathbf{h}_2 \tag{2.40}$$

$$= (\mathbf{I}_{M_0} \otimes \mathbf{h}_2)\,\mathbf{h}_1, \tag{2.41}$$

where $\mathbf{I}_{M_0}$ is the $M_0 \times M_0$ identity matrix. Basically, the previous expressions, which separate $\mathbf{h}_2$ and $\mathbf{h}_1$ into matrix-vector products, will often be very helpful and convenient to use in the derivation of beamformers.

When $\mathbf{h}_2$ is fixed, given, and satisfies the distortionless constraint, i.e., $\mathbf{h}_2^H \mathbf{d}_{2,\theta_\mathrm{d}} = 1$; then, thanks to (2.41), we can write the DF as

$$\mathcal{D}\left(\mathbf{h}_1|\mathbf{h}_2\right) = \frac{\left|\mathcal{B}_{1,\theta_\mathrm{d}}\left(\mathbf{h}_1\right)\right|^2}{\mathbf{h}_1^H \boldsymbol{\Gamma}_{\mathbf{h}_2} \mathbf{h}_1} = \frac{\left|\mathbf{h}_1^H \mathbf{d}_{1,\theta_\mathrm{d}}\right|^2}{\mathbf{h}_1^H \boldsymbol{\Gamma}_{\mathbf{h}_2} \mathbf{h}_1}, \tag{2.42}$$

where

$$\begin{aligned}\boldsymbol{\Gamma}_{\mathbf{h}_2} &= \frac{1}{2}\int_0^\pi \mathbf{d}_{1,\theta}\mathbf{d}_{1,\theta}^H \left|\mathcal{B}_{2,\theta}\left(\mathbf{h}_2\right)\right|^2 \sin\theta d\theta \\ &= \left(\mathbf{I}_{M_0} \otimes \mathbf{h}_2\right)^H \boldsymbol{\Gamma} \left(\mathbf{I}_{M_0} \otimes \mathbf{h}_2\right).\end{aligned} \tag{2.43}$$

In the same way, when $\mathbf{h}_1$ is fixed, given, and satisfies the distortionless constraint, i.e., $\mathbf{h}_1^H \mathbf{d}_{1,\theta_\mathrm{d}} = 1$; then, thanks to (2.40), we can express the DF as

$$\mathcal{D}\left(\mathbf{h}_2|\mathbf{h}_1\right) = \frac{\left|\mathcal{B}_{2,\theta_\mathrm{d}}\left(\mathbf{h}_2\right)\right|^2}{\mathbf{h}_2^H \boldsymbol{\Gamma}_{\mathbf{h}_1} \mathbf{h}_2} = \frac{\left|\mathbf{h}_2^H \mathbf{d}_{2,\theta_\mathrm{d}}\right|^2}{\mathbf{h}_2^H \boldsymbol{\Gamma}_{\mathbf{h}_1} \mathbf{h}_2}, \tag{2.44}$$

where

$$\begin{aligned}\boldsymbol{\Gamma}_{\mathbf{h}_1} &= \frac{1}{2}\int_0^\pi \mathbf{d}_{2,\theta}\mathbf{d}_{2,\theta}^H \left|\mathcal{B}_{1,\theta}\left(\mathbf{h}_1\right)\right|^2 \sin\theta d\theta \\ &= \left(\mathbf{h}_1 \otimes \mathbf{I}_{M_0}\right)^H \boldsymbol{\Gamma} \left(\mathbf{h}_1 \otimes \mathbf{I}_{M_0}\right).\end{aligned} \tag{2.45}$$

References

1. B. D. Van Veen and K. M. Buckley, "Beamforming: a versatile approach to spatial filtering," *IEEE Acoust., Speech, Signal Process. Mag.*, vol. 5, pp. 4–24, Apr. 1988.
2. D. H. Johnson and D. E. Dudgeon, *Array Signal Processing: Concepts and Techniques*. Signal Processing Series. Englewood Cliffs, NJ: Prentice-Hall, 1993.
3. J. Benesty, J. Chen, and Y. Huang, *Microphone Array Signal Processing*. Berlin, Germany: Springer-Verlag, 2008.
4. J. Benesty, I. Cohen, and J. Chen, *Fundamentals of Signal Enhancement and Array Signal Processing*. Singapore: Wiley–IEEE Press, 2018.
5. Y. I. Abramovich, G. J. Frazer, and B. A. Johnson, "Iterative adaptive Kronecker MIMO radar beamformer: description and convergence analysis," *IEEE Trans. Signal Process.*, vol. 58, pp. 3681–3691, Jul. 2010.
6. H. L. Van Trees, *Optimum Array Processing: Part IV of Detection, Estimation, and Modulation Theory*. New York, NY: John Wiley & Sons, Inc., 2002.

Chapter 3
Beamforming with Uniform Linear Arrays

Any good microphone array system requires a reliable beamforming algorithm at the outputs of the sensors to enhance a desired signal coming from a known direction. There are many ways to optimize the coefficients of this beamformer depending on what we want and the application at hand. Fundamentally, there are three large classes of conventional beamformers; they are the fixed, adaptive, and differential beamformers. In this chapter, we show how to derive most of their counterparts as well as new approaches with Kronecker product filters. We also show how to combine fixed and adaptive beamforming. While most of these beamformers are rather easy to derive, for some it is necessary to use iterative algorithms. The focus is on ULAs and with the decomposition of the steering vector of Chapter 2.

3.1 Fixed Beamformers

In this first section, we derive many examples of fixed beamformers thanks to the Kronecker product decomposition. We start with the most obvious one.

3.1.1 Delay and Sum

The most well-known and popular fixed beamformer is the so-called delay and sum (DS), which is derived by maximizing the WNG. Given the structure of the WNG of $\mathbf{h}$, it is clear that the maximization of this gain is equivalent to maximizing $\mathcal{W}_1(\mathbf{h}_1)$ and $\mathcal{W}_2(\mathbf{h}_2)$ separately. Taking into account the distortionless constraints, we easily get the DS beamformers at the two subarrays:

J. Benesty et al., *Array Processing*, Springer Topics in Signal Processing 18, https://doi.org/10.1007/978-3-030-15600-8_3

$$\mathbf{h}_{1,\mathrm{DS}} = \frac{\mathbf{d}_{1,\theta_\mathrm{d}}}{M_0}, \tag{3.1}$$

$$\mathbf{h}_{2,\mathrm{DS}} = \frac{\mathbf{d}_{2,\theta_\mathrm{d}}}{M_0}. \tag{3.2}$$

As a consequence, the DS beamformer corresponding to the global ULA is

$$\begin{aligned}\mathbf{h}_{\mathrm{DS}} &= \mathbf{h}_{1,\mathrm{DS}} \otimes \mathbf{h}_{2,\mathrm{DS}} \\ &= \frac{\mathbf{d}_{1,\theta_\mathrm{d}} \otimes \mathbf{d}_{2,\theta_\mathrm{d}}}{M_0^2} \\ &= \frac{\mathbf{d}_{\theta_\mathrm{d}}}{M_0^2},\end{aligned} \tag{3.3}$$

which is, of course, the classical DS beamformer [1], [2]. Here, however, it is shown how the structure of the global steering vector is exploited. In other words, the DS beamformer is determined by $2M_0$ different coefficients only when $M = M_0^2$.

It is obvious that

$$\mathcal{W}\left(\mathbf{h}_{\mathrm{DS}}\right) = M_0^2 = M \tag{3.4}$$

and the beampattern of the DS beamformer is

$$\begin{aligned}\mathcal{B}_\theta\left(\mathbf{h}_{\mathrm{DS}}\right) &= \mathcal{B}_{1,\theta}\left(\mathbf{h}_{1,\mathrm{DS}}\right) \times \mathcal{B}_{2,\theta}\left(\mathbf{h}_{2,\mathrm{DS}}\right) \\ &= \frac{1}{M_0^2}\left(\mathbf{d}_{1,\theta}^H \mathbf{d}_{1,\theta_\mathrm{d}}\right)\left(\mathbf{d}_{2,\theta}^H \mathbf{d}_{2,\theta_\mathrm{d}}\right).\end{aligned} \tag{3.5}$$

Finally, the DF of $\mathbf{h}_{\mathrm{DS}}$ is

$$\mathcal{D}\left(\mathbf{h}_{\mathrm{DS}}\right) = \frac{M_0^4}{\mathbf{d}_{\theta_\mathrm{d}}^H \boldsymbol{\Gamma} \mathbf{d}_{\theta_\mathrm{d}}}. \tag{3.6}$$

3.1.2 Partial Maximum DF

There are different fixed beamformers for which the DF is only maximized in part. We review some possibilities.

In the first approach, we assume that $\mathbf{h}_2$ is fixed. We may take $\mathbf{h}_2 = \mathbf{h}_{2,\mathrm{DS}}$ for the second ULA. Substituting this filter into (2.42), we get

$$\mathcal{D}\left(\mathbf{h}_1 | \mathbf{h}_{2,\mathrm{DS}}\right) = \frac{\left|\mathbf{h}_1^H \mathbf{d}_{1,\theta_\mathrm{d}}\right|^2}{\mathbf{h}_1^H \boldsymbol{\Gamma}_{\mathbf{h}_{2,\mathrm{DS}}} \mathbf{h}_1}, \tag{3.7}$$

where

$$\mathbf{\Gamma}_{\mathbf{h}_{2,\mathrm{DS}}} = \left(\mathbf{I}_{M_0} \otimes \mathbf{h}_{2,\mathrm{DS}}\right)^H \mathbf{\Gamma} \left(\mathbf{I}_{M_0} \otimes \mathbf{h}_{2,\mathrm{DS}}\right). \tag{3.8}$$

The maximization of $\mathcal{D}\left(\mathbf{h}_1|\mathbf{h}_{2,\mathrm{DS}}\right)$ gives the maximum DF beamformer at the first ULA:

$$\mathbf{h}_{1,\mathrm{mDF1}} = \frac{\mathbf{\Gamma}_{\mathbf{h}_{2,\mathrm{DS}}}^{-1}\mathbf{d}_{1,\theta_\mathrm{d}}}{\mathbf{d}_{1,\theta_\mathrm{d}}^H\mathbf{\Gamma}_{\mathbf{h}_{2,\mathrm{DS}}}^{-1}\mathbf{d}_{1,\theta_\mathrm{d}}}. \tag{3.9}$$

Therefore, our first (global) partial maximum DF (PmDF) beamformer is

$$\mathbf{h}_{\mathrm{PmDF1}} = \mathbf{h}_{1,\mathrm{mDF1}} \otimes \mathbf{h}_{2,\mathrm{DS}}. \tag{3.10}$$

We deduce that the WNG and the beampattern are, respectively,

$$\mathcal{W}\left(\mathbf{h}_{\mathrm{PmDF1}}\right) = M_0\mathcal{W}\left(\mathbf{h}_{1,\mathrm{mDF1}}\right) \tag{3.11}$$

and

$$\mathcal{B}_\theta\left(\mathbf{h}_{\mathrm{PmDF1}}\right) = \mathcal{B}_{1,\theta}\left(\mathbf{h}_{1,\mathrm{mDF1}}\right) \times \mathcal{B}_{2,\theta}\left(\mathbf{h}_{2,\mathrm{DS}}\right). \tag{3.12}$$

Figure 3.1 displays the directivity patterns of the first partial maximum DF beamformer, $\mathbf{h}_{\mathrm{PmDF1}}$, for $\theta_\mathrm{d} = 0$, $f = 1$ kHz, $\delta = 1$ cm, and different numbers of sensors $M = M_0^2$. Figure 3.2 shows plots of the DFs and WNGs of the first partial maximum DF beamformer as a function of frequency for $\theta_\mathrm{d} = 0$, $\delta = 1$ cm, and different numbers of sensors. We observe that as the number of sensors increases, the width of the main beam and the level of side lobes decrease, while the DF of the first partial maximum DF beamformer increases. However, using a larger number of sensors increases the WNG of the first partial maximum DF beamformer only for high frequencies, but decreases its WNG for low frequencies.

In the second approach, we assume that $\mathbf{h}_1$ is fixed, i.e., $\mathbf{h}_1 = \mathbf{h}_{1,\mathrm{DS}}$ for the first ULA. Substituting this filter into (2.44), we get

$$\mathcal{D}\left(\mathbf{h}_2|\mathbf{h}_{1,\mathrm{DS}}\right) = \frac{\left|\mathbf{h}_2^H\mathbf{d}_{2,\theta_\mathrm{d}}\right|^2}{\mathbf{h}_2^H\mathbf{\Gamma}_{\mathbf{h}_{1,\mathrm{DS}}}\mathbf{h}_2}, \tag{3.13}$$

where

$$\mathbf{\Gamma}_{\mathbf{h}_{1,\mathrm{DS}}} = \left(\mathbf{h}_{1,\mathrm{DS}} \otimes \mathbf{I}_{M_0}\right)^H \mathbf{\Gamma} \left(\mathbf{h}_{1,\mathrm{DS}} \otimes \mathbf{I}_{M_0}\right). \tag{3.14}$$

The maximization of $\mathcal{D}\left(\mathbf{h}_2|\mathbf{h}_{1,\mathrm{DS}}\right)$ gives the maximum DF beamformer at the second ULA:

$$\mathbf{h}_{2,\mathrm{mDF2}} = \frac{\mathbf{\Gamma}_{\mathbf{h}_{1,\mathrm{DS}}}^{-1}\mathbf{d}_{2,\theta_\mathrm{d}}}{\mathbf{d}_{2,\theta_\mathrm{d}}^H\mathbf{\Gamma}_{\mathbf{h}_{1,\mathrm{DS}}}^{-1}\mathbf{d}_{2,\theta_\mathrm{d}}}. \tag{3.15}$$

As a result, our second partial maximum DF beamformer is

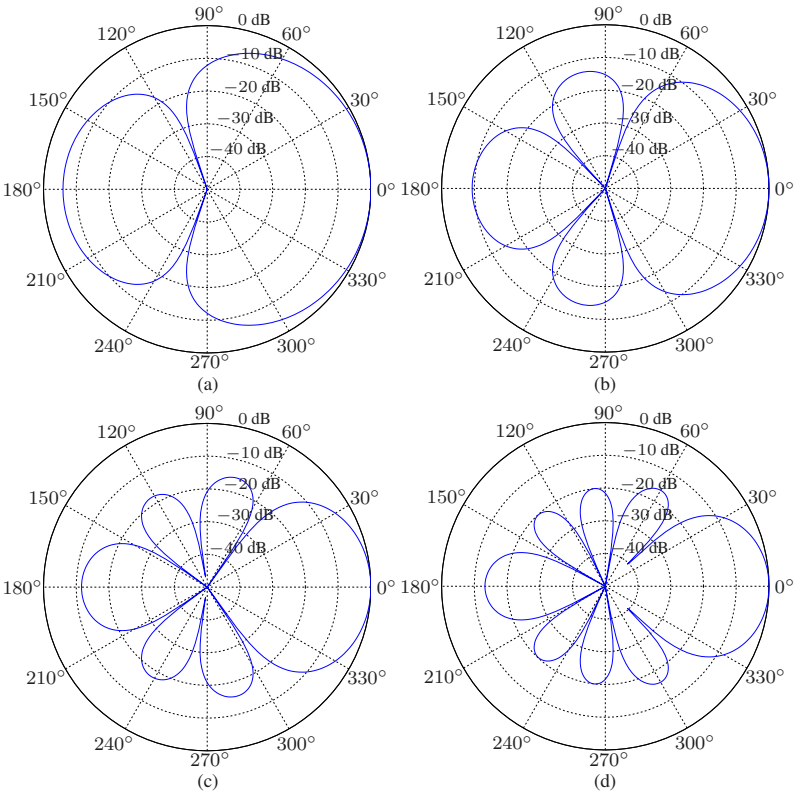

Fig. 3.1 Beampatterns of the first partial maximum DF beamformer, $\mathbf{h}_{\mathrm{PmDF1}}$, for $\theta_{\mathrm{d}} = 0$, $f = 1$ kHz, $\delta = 1$ cm, and different numbers of sensors $M = M_0^2$: (a) $M_0 = 2$, (b) $M_0 = 3$, (c) $M_0 = 4$, and (d) $M_0 = 5$.

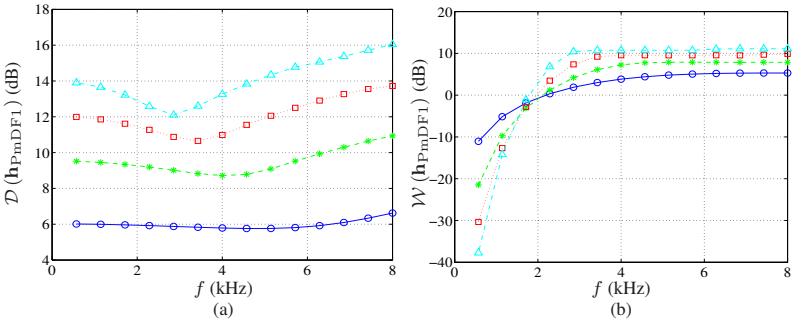

Fig. 3.2 Performance of the first partial maximum DF beamformer, $\mathbf{h}_{\mathrm{PmDF1}}$, as a function of frequency for $\theta_{\mathrm{d}} = 0$, $\delta = 1$ cm, and different numbers of sensors $M = M_0^2$: $M_0 = 2$ (solid line with circles), $M_0 = 3$ (dashed line with asterisks), $M_0 = 4$ (dotted line with squares), and $M_0 = 5$ (dash-dot line with triangles). (a) DF and (b) WNG.